

Nighttime Smartphone Reflective Flare Removal Using Optical Center Symmetry Prior (Supplementary Material)

Yuekun Dai Yihang Luo Shangchen Zhou Chongyi Li* Chen Change Loy
S-Lab, Nanyang Technological University

{YDAI005, c200211, s200094, chongyi.li, ccloy}@ntu.edu.sg

A. Comparison with Previous Pipelines

To prove the performance of our dataset, we retrain Wu *et al.* [7] and Dai *et al.* [2] on our BracketFlare dataset and conduct additional experiments as shown in Table 1. Wu *et al.* [7] use U-Net as a baseline model, but we find it struggled to locate reflective flares without our prior, sometimes reducing PSNR compared to the input. Dai *et al.* [2] set Uformer as a baseline. Since it does not encode the prior into the network, it has an obvious gap between our baseline method. To show these methods’ effects on real data, we also conduct a user study with 20 real-captured flare-corrupted images and 20 participants. The participants are asked to identify which of these models did best at removing the reflective flares. The experiments presented in Table 2 illustrates that users strongly prefer our methods over previous methods.

Table 1. Comparison of previous models retrained on our dataset.

Model (Retrained)	PSNR	SSIM	LPIPS	Masked PSNR
Input	37.30	0.990	0.025	21.68
Wu et al. [7]	31.84	0.912	0.032	24.87
Dai et al. [2]	42.70	0.987	0.010	27.46
Ours	48.41	0.994	0.004	32.09

B. Flare Removal for Downstream Tasks

Fig. 1 demonstrates that it can benefit downstream tasks such as image segmentation. In the figure, it can be observed that the reflective flares are misclassified as a pole, which may pose potential risks for nighttime driving. Removing such reflective flares can help achieve more robust and reliable results, and ultimately benefit the users.

C. Potential in Overexposure Restoration

Due to the limited dynamic range of some cameras, image details especially in light source regions are always saturated and difficult to recover. To achieve the details of

*Corresponding author.

Table 2. Percentage of users favoring our method and other re-trained models.

Method	Wu et al. [7]	Dai et al. [2]	Ours
Indoor	0.5%	3.5%	96%
Outdoor	1.5%	2.5%	96%

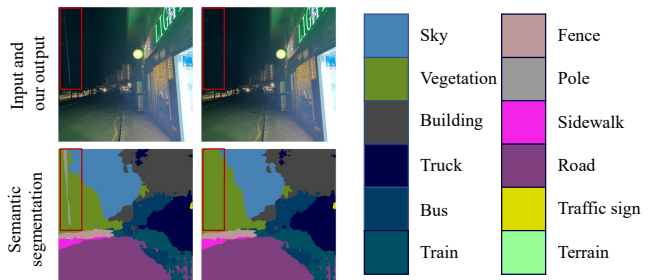


Figure 1. Visual comparison of estimated segmentation for real-world flare-corrupted and flare-removed image pairs. The segmentation maps are calculated by DANNet [6], a nighttime semantic segmentation algorithm.

the overexposed regions, the mainstream solution is to use HDR (high-dynamic range) imaging with multi-exposure capture [3, 4]. Our main idea may provide a potential solution to this issue.

Specifically, since smartphone reflective flare can be considered as a short-exposure image, our method also provides the potential in implementing overexposed regions restoration. As shown in Fig. 2, we can separate a reflective flare and rotate the estimated flare 180 degrees around the optical center to match the flare with the light source. We suppose the exposure step between the flare and the original input is 12 EV. Then, these two images with low-dynamic ranges will be merged to generate an HDR image with clear details in the light source. The visualization results in Fig. 2 show that our method can recover the details of the saturated regions well.

D. More Visual Results

To further demonstrate the effectiveness of our dataset, we retrain different neural networks including Uformer [5],

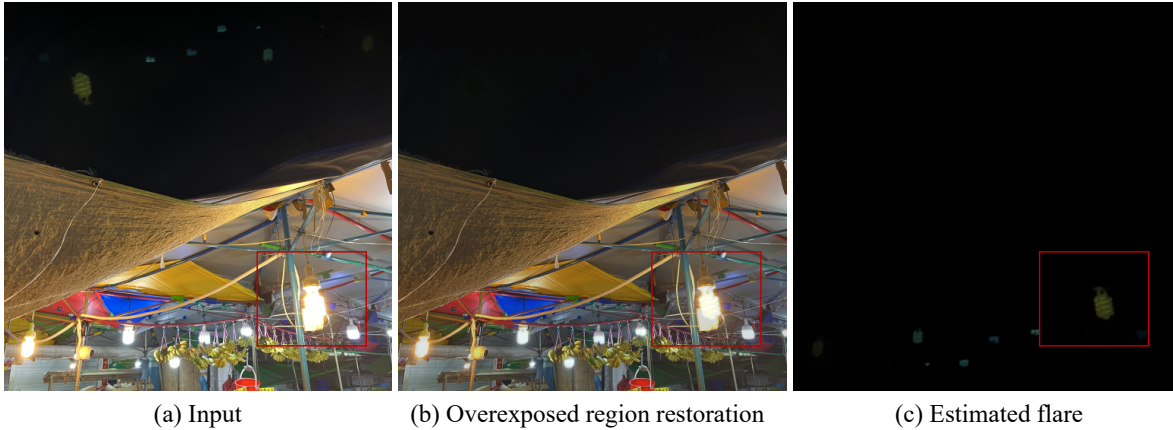


Figure 2. Our reflective flare removal method can help achieve overexposed region restoration. As shown in (c), the details of the light source can be reconstructed well by referring to the estimated flare.

Restormer [8], HINet [1], and MPRNet [9] using our proposed dataset. The visual results of different networks for restoring real-world images are presented in Fig. 3. From the visual comparison, we can observe that all the networks retrained on our dataset can remove the flares. Among them, MPRNet [9] obtains the best performance on flare-corrupted regions, as highlighted in the red boxes of Fig. 3. The results manifest the effectiveness of our proposed dataset.

To show our dataset and prior’s generalization ability in different real-world scenes, we show more results of the flare-corrupted images captured by iPhone 13 Pro that is known for severe reflective flares in Fig. 4 and Fig. 5. The results show that our proposed method can tackle a huge diversity of light sources and achieve good visual performance in different scenes. It is owing to the versatility of our proposed prior, as well as the diversity and balanced distribution of our proposed dataset.

We also capture many flare-corrupted video clips by Huawei P40, iPhone 13 Pro, and ZTE Axon 20 5G. To prevent triggering the anti-shake module of the smartphone, we try to keep the smartphone from large movement. Then, we process these videos with our method frame by frame. The video results can be found in a separate video demo. The video demo shows that our method can achieve robust and consistent flare-removal results even for real-world videos.

E. Limitation

As shown in Fig. 10 of the main paper, our method can generalize well to different types of smartphones. However, it is based on the fact that most smartphone cameras satisfy the optical center symmetry prior. For some professional cameras, this prior does not always hold. Besides, due to the dispersion of thick lenses in professional cameras, the main flare spot of the professional cameras are not always

the same as the light source’s pattern. The solutions for these cases will be left for future work.

References

- [1] Liangyu Chen, Xin Lu, Jie Zhang, Xiaojie Chu, and Chengpeng Chen. Hinet: Half instance normalization network for image restoration. In *CVPRW*, 2021. 2, 3
- [2] Yuekun Dai, Chongyi Li, Shangchen Zhou, Ruicheng Feng, and Chen Change Loy. Flare7k: A phenomenological nighttime flare removal dataset. In *Thirty-sixth Conference on Neural Information Processing Systems Datasets and Benchmarks Track*, 2022. 1
- [3] Paul E Debevec and Jitendra Malik. Recovering high dynamic range radiance maps from photographs. In *ACM SIGGRAPH*, 2008. 1
- [4] Erik Reinhard, Wolfgang Heidrich, Paul Debevec, Sumanta Pattanaik, Greg Ward, and Karol Myszkowski. *High dynamic range imaging: acquisition, display, and image-based lighting*. Morgan Kaufmann, 2010. 1
- [5] Zhendong Wang, Xiaodong Cun, Jianmin Bao, Wengang Zhou, Jianzhuang Liu, and Houqiang Li. Uformer: A general u-shaped transformer for image restoration. In *CVPR*, 2022. 1, 3
- [6] Xinyi Wu, Zhenyao Wu, Hao Guo, Lili Ju, and Song Wang. Danner: A one-stage domain adaptation network for unsupervised nighttime semantic segmentation. In *CVPR*, 2021. 1
- [7] Yicheng Wu, Qiurui He, Tianfan Xue, Rahul Garg, Jiawen Chen, Ashok Veeraraghavan, and Jonathan T Barron. How to train neural networks for flare removal. In *ICCV*, 2021. 1
- [8] Syed Waqas Zamir, Aditya Arora, Salman Khan, Munawar Hayat, Fahad Shahbaz Khan, and Ming-Hsuan Yang. Restormer: Efficient transformer for high-resolution image restoration. In *CVPR*, 2022. 2, 3
- [9] Syed Waqas Zamir, Aditya Arora, Salman Khan, Munawar Hayat, Fahad Shahbaz Khan, Ming-Hsuan Yang, and Ling Shao. Multi-stage progressive image restoration. In *CVPR*, 2021. 2, 3, 4, 5

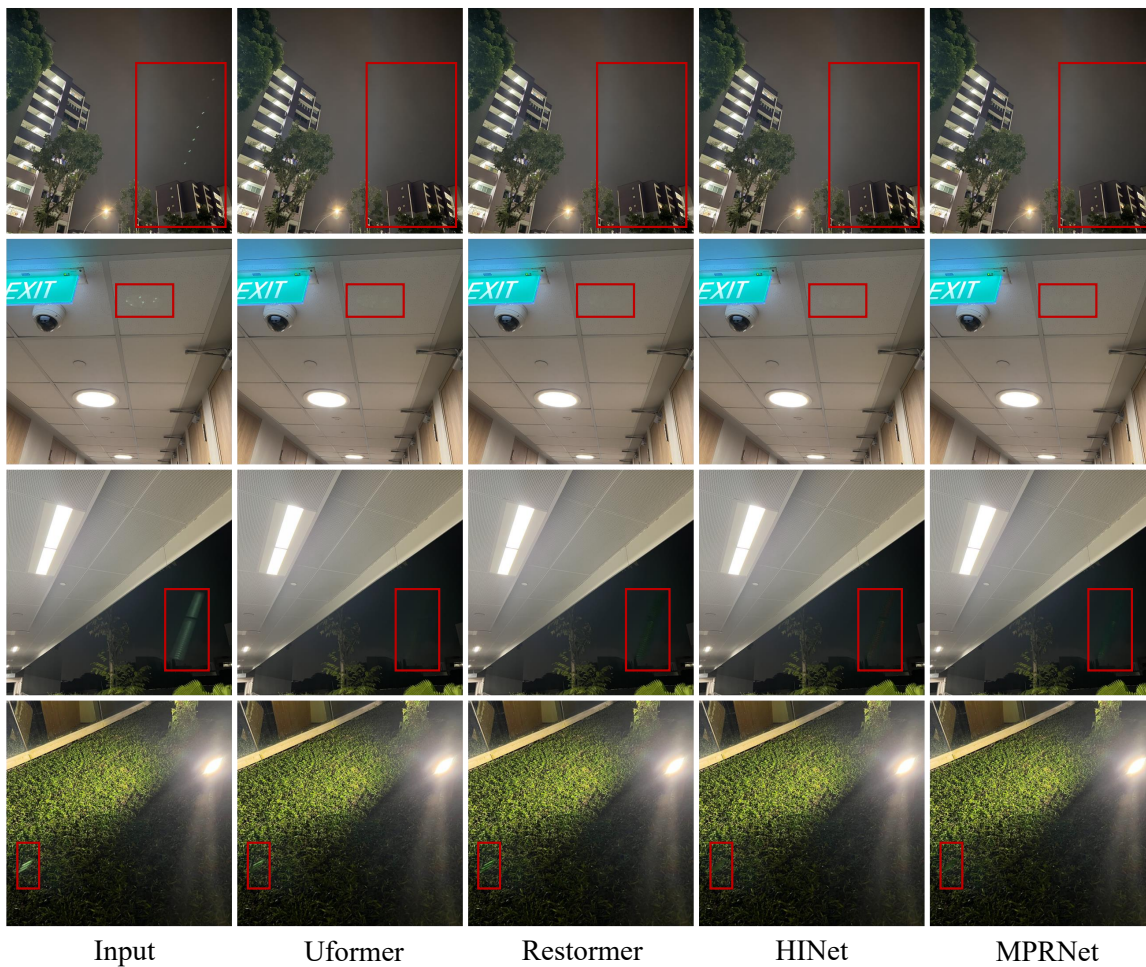


Figure 3. Visual comparison of different networks retrained on our dataset for restoring the real-world flare-corrupted images. These image restoration networks include Uformer [5], Restormer [8], HINet [1], and MPRNet [9].

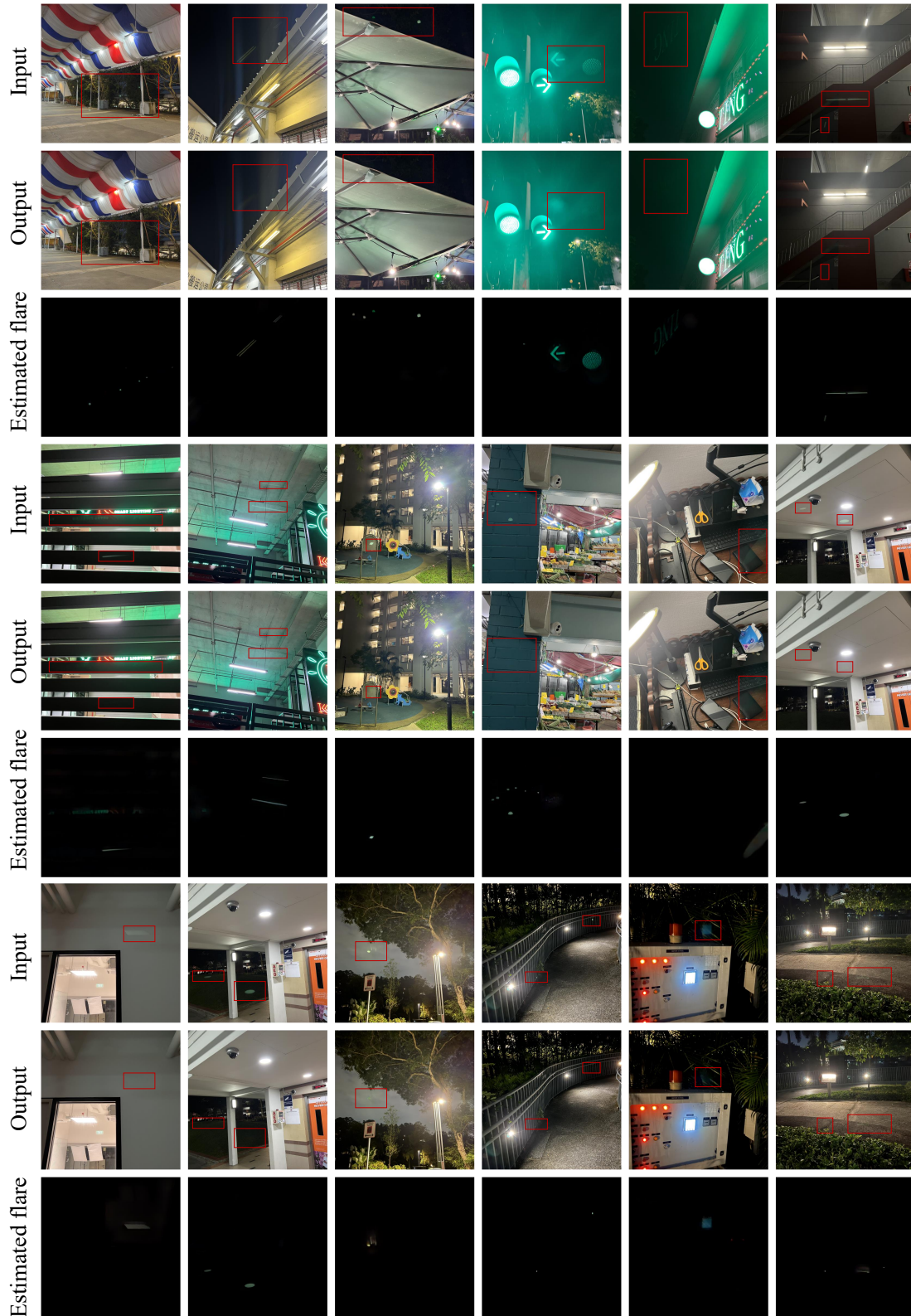


Figure 4. Our results on real-world nighttime flare-corrupted images. In this figure, we use MPRNet [9] as the baseline method to estimate the flare and output image.

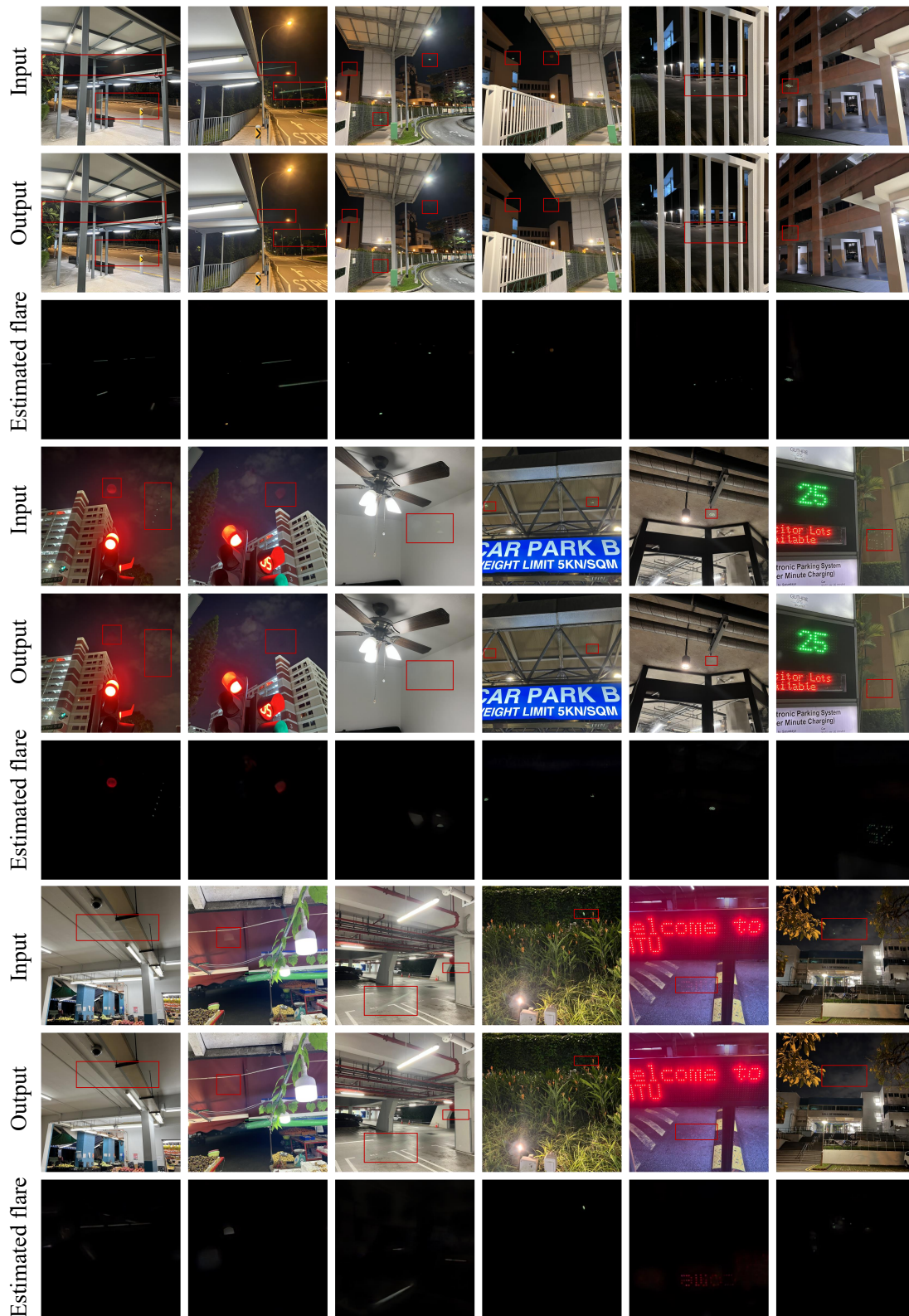


Figure 5. More results on real-world nighttime flare-corrupted images. In this figure, We use MPRNet [9] as the baseline method to estimate the flare and output image.